Phase transition of tetragonal copper sulfide Cu_2S at low temperatures

D. Zimmer,[1,*] J. Ruiz-Fuertes,[2] L. Bayarjargal,[1] E. Haussühl,[1] B. Winkler,[1] J. Zhang,[3] C. Q. Jin,[3] V. Milman,[4] E. Alig,[5] and L. Fink[5]

[1]*Institute of Geosciences, Goethe-University Frankfurt, 60438 Frankfurt am Main, Germany*

[2]*Departament de Física Aplicada-ICMUV, Universitat de València, 46100 Burjassot, Spain*

[3]*The Institute of Physics, Chinese Academy of Sciences, 100190 Beijing, China*

[4]*Dassault Systèmes BIOVIA, CB4 0WN Cambridge, United Kingdom*

[5]*Institute of Inorganic and Analytical Chemistry, Goethe-University Frankfurt, 60438 Frankfurt am Main, Germany*

(Received 10 July 2017; published 11 August 2017)

The low-temperature behavior of tetragonal copper sulfide, Cu_2S, was investigated by powder and single-crystal x-ray diffraction, calorimetry, electrical resistance measurements, and ambient temperature optical absorption spectroscopy. The experiments were complemented by density-functional-theory-based calculations. High-quality, polycrystalline samples and single crystals of tetragonal copper sulfide were synthesized at 5 GPa and 700 K in a large volume multianvil press. Tetragonal Cu_2S undergoes a temperature-induced phase transition to an orthorhombic structure at around 202 K with a hysteresis of ±21 K, an enthalpy of reaction of 1.3(2) kJ mol^{-1}, and an entropy of reaction of 6.5(2) J mol^{-1} K^{-1}. The temperature dependence of the heat capacity at the transition temperature indicates that the transition from the tetragonal to the low-temperature polymorph is not a single process. The structure of the low-temperature polymorph at 100 K was solved in space group $Pna2_1$. The structure is based on a slightly distorted cubic close packing of sulfur with copper in threefold coordination similar to the structure of tetragonal copper sulfide. The electrical resistance changes several orders of magnitude at the transition following the temperature hysteresis. The activation energy of the conductivity for the tetragonal phase and the low-temperature polymorph are 0.15(2) and 0.22(1) eV, respectively. The direct band gap of the tetragonal polymorph is found to be 1.04(2) eV with the absorption spectrum following Urbach's law. The activation energies and the band gaps of both phases are discussed with respect to the results of the calculated electronic band structures.

DOI: 10.1103/PhysRevB.96.054108

I. INTRODUCTION

Copper sulfides, Cu_xS, are a family of compounds with outstanding physical properties such as ion conductivity [1], *p*-type semiconductivity [1], superconductivity [2], thermoelectricity [3], and fast switchable phase transitions [4] resulting in a wide field of potential industrial applications reaching from thin film solar cell absorbers [5] to resistive switching devices [6]. Due to the high mobility of copper within the sulfur sublattice the structural phase relations are complex even at ambient conditions and have therefore been in the focus of numerous studies since 1926 [7,8]. Up to now six phases have been found to be stable or at least metastable at ambient conditions with compositions between Cu_2S and $Cu_{1.75}S$: chalcocite [9], djurleite [10], roxbyite [11], digenite [12], anilite [13], and tetragonal copper sulfide [14]. The rapidly growing research on nanocrystalline materials increased the interest in copper chalcogenides further [15]. In recent studies tetragonal copper sulfide nanocrystals were found to be potentially useful for highly efficient quantum-dot-sensitized solar cells [16]. However, apart from this study our knowledge of the properties of tetragonal copper sulfide is rather limited and inconsistent.

A tetragonal copper sulfide [$a = 4.008(2)$ Å, $c = 11.268(6)$ Å] with a stoichiometry of $Cu_{1.96}S$ was first described by Djurle [14] as a high-temperature polymorph of a low-symmetric phase (today known as the mineral djurleite [10]). This compound can be recovered metastably at ambient conditions. Roseboom, Jr. [17] proposed that the tetragonal phase is stable in a compositional range of ~Cu_2S to $Cu_{1.96}S$. Skinner [18] showed that tetragonal copper sulfide is stable at elevated pressures and temperatures as a polymorph of monoclinic Cu_2S, α-chalcocite [9]. Skinner [18] also stated that at ambient temperature and at 271 K the rates of conversion of tetragonal copper sulfide into α-chalcocite are about 1% and 0.2% per day, respectively.

The structure of this tetragonal polymorph was solved and described by Janosi [20] in space group $P4_32_12$ with $a = 3.996(2)$ Å, $c = 11.28(7)$ Å, and $Z = 4$ using powder x-ray diffraction data. The structure can be described by sixfold coordinated sulfur atoms forming a slightly distorted cubic close packing with copper in trigonal coordination as shown in Fig. 1.

Pakeva and Germanova [21] performed resistance measurements between 90 and 300 K on polycrystalline copper sulfide samples containing mainly tetragonal copper sulfide in addition to four other modifications finding no indication for a temperature-induced phase transition. In contrast Stolen *et al.* [22] performed heat capacity measurements on copper sulfide samples with a stoichiometry of $Cu_{1.95}S$ containing small amounts of the tetragonal phase and found an anomaly in the heat capacity as a function of temperature around 220 K, showing a hysteresis. Using x-ray diffraction Stolen *et al.* [22] concluded that the tetragonal copper sulfide undergoes a structural phase transition at this temperature, but they were only able to identify five reflections disappearing above the transition temperature and were not able to index the reflections of the new low-temperature polymorph.

*zimmer@kristall.uni-frankfurt.de

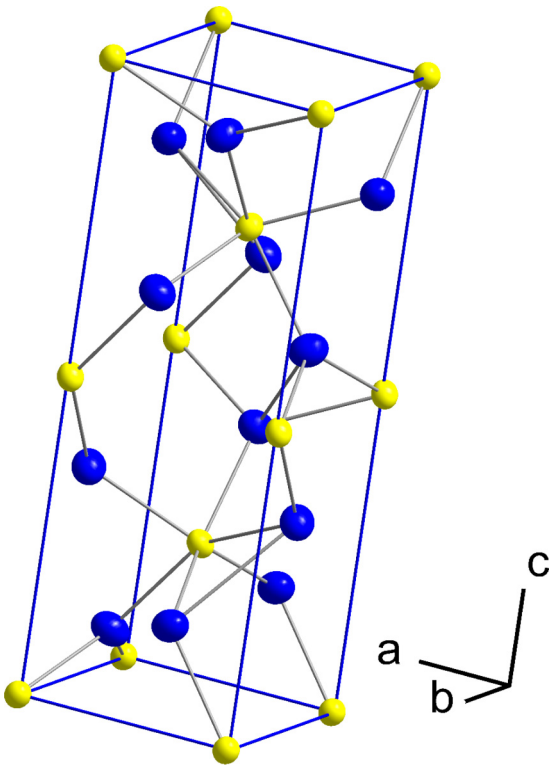

FIG. 1. Crystal structure of tetragonal copper sulfide based on single-crystal x-ray diffraction data [19]. Yellow: sulfur; blue: copper.

Monoclinic α-chalcocite, Cu_2S, has been proposed for the development of Cu_2S:CdS thin-film cells for photovoltaics due to its appropriate optical properties [5,23]. But its limited phase stability has prevented its deployment in real applications up to now [24,25]. However, recently synthesized tetragonal copper sulfide nanoparticles, which have similar optical properties to the monoclinic polymorph, have been shown to be stable to high temperatures [26]. Therefore, it is now of interest to establish the structure-property relations of tetragonal Cu_2S, so that a benchmark is available which allows us to quantify improvements of the stability and properties.

The aim of this study is therefore to clarify the low-temperature behavior of tetragonal copper sulfide using phase-pure samples and to investigate structural and physical properties of tetragonal copper sulfide and the low-temperature polymorph.

II. EXPERIMENTAL DETAILS

Tetragonal copper sulfide was synthesized from the elements in the form of powders (copper: 99,99% 150 μm, ChemPUR, Karlsruhe; sulfur: 99,99%, Sigma-Aldrich, Missouri) at 700 K and 5 GPa with copper in excess to prevent the formation of digenite ($Cu_{2-x}S$) [27]. The synthesis conditions were generated in a resistive-heated, large volume multianvil press at the Chinese Academy of Sciences in Beijing using gold capsules as sample chambers embedded in sodium chloride as pressure transmitting medium. The samples were stored in a freezer at temperatures below 260 K and were not exposed to ambient temperature longer than 1 hour before any experiment to prevent any transformation into α-chalcocite.

Characterization of the samples was performed by powder x-ray diffraction with a STOE Stadi P diffractometer equipped with a linear position-sensitive detector and a bent Ge(111)-monochromator using Cu $K\alpha_1$ radiation. For diffraction experiments at ~100 K a nitrogen stream was used provided by a Cryostream 700 from Oxford Cryosystems. Data were collected in a 2Θ range from 3° to 100° with a step width of 0.01° and a measurement time of ~120 minutes per step. Rietveld refinements [28] were executed by employing GSAS [29] with the EXPGUI [30] package.

Single-crystal x-ray diffraction was performed at ambient conditions and 100 K using an Xcalibur3 four-circle diffractometer from Oxford diffraction equipped with graphite-monochromatized Mo $K\alpha$ radiation and a charge coupled device camera (Sapphire3). The sample was mounted on the goniometer head with a distance of 42 mm with respect to the detector. For low-temperature measurements a cryostream system from Oxford diffraction was employed generating 100 K with an error of 5 K. At ambient temperature 365 frames were collected with a scan width of 1° and an exposure time of 90 s. At 100 K 518 frames were collected with a scan width of 0.7° and an exposure time of 125 s. For indexing, data reduction and empirical absorption correction the CRYSALIS^{Pro} software Agilent [31] was employed. Structure solution and structural refinements were performed using SUPERFLIP [32] and JANA2006 [33], respectively.

The electrical properties of tetragonal copper sulfide were determined by four-wire resistance measurements between 300 and 150 K using a Quantum Design physical properties measurement system. Electrical contact between the four copper wires and the sample was established by silver-based conductive varnish. At each temperature step 25 resistance measurements were performed. The results were used to calculate the mean and standard deviation. Possible errors due to thermoelectric effects were avoided by alternating the direction of the excitation current.

The heat capacity of tetragonal copper sulfide was determined by differential scanning calorimetry (DSC) between 120 and 240 K using a Netzsch DSC 204 F1 Phoenix. For all measurements the heating and cooling rate was set to 4 K/min and helium was used as protective gas. To establish sufficient thermal contact between the platinum crucibles and the compact copper sulfide the largest side of the samples was polished and cleaned before the measurement. To determine the measurement background and for calibration an empty crucible and a sapphire disk were measured prior to every measurement of a sample, respectively. From the measured heat capacity data the molar enthalpy of reaction ΔH_{reac} and the molar entropy of reaction S_{reac} were calculated using the following equations:

$$\Delta H_{reac} = \int_{T_1}^{T_2} C_p \, dT \tag{1}$$

and

$$S_{reac} = \int_{T_1}^{T_2} \frac{C_p}{T} \, dT \tag{2}$$

by subtracting the background from the reaction peaks and integrating the data numerically.

Relaxation calorimetry was performed using a Quantum Design thermal relaxation calorimeter [physical properties measurement system (PPMS)]. The thermal contact between the flat sample surface and the sample holder was ensured by using Apiezon-N grease. The compact samples of a few milligrams mass were measured in a temperature range between 300 and 2 K. Based on the two-τ model, the heat capacity was determined three times at each temperature point [34]. The two-τ model is only valid if the change of heat capacity within the relaxation interval is small, which is not the case at the first-order phase transition we observe in tetragonal copper sulfide. Therefore, the measured heat capacities in the temperature range of the phase transition were omitted from the analysis and instead a fit of the temperature dependence of the heat capacity was employed for the interpolation in this temperature interval. For the calculation of the standard molar entropy S^0 the value for the entropy of reaction derived from DSC measurements was added to the value calculated from the extrapolated fit using Eq. (2). The Debye temperature θ_D in [K] was calculated using

$$C_V = \frac{12\pi^4}{5} nR\left(\frac{T^3}{\theta_D^3}\right) \tag{3}$$

under the assumption that the difference between C_p and C_V is negligible, where C_V is the isochoric heat capacity in [J K^{-1}], n is the amount of substance in [mol], R is the gas constant in [J mol^{-1} K^{-1}], and T is the absolute temperature in [K].

Optical absorption measurements were performed in a custom-built confocal system equipped with two Cassegrain objectives and a halogen lamp. The spectrometer used was a NIR StellarNet equipped with an InGaAs detector.

III. COMPUTATIONAL DETAILS

First-principles calculations were carried out within the framework of density-functional theory (DFT) [35] and the pseudopotential method using the CASTEP [36] simulation package. "On the fly" ultrasoft pseudopotentials from the CASTEP data base were employed in conjunction with plane waves up to a kinetic energy cutoff of 450 eV. A Monkhorst-Pack [37] grid was used for Brillouin-zone integrations with a distance of <0.012 Å^{-1} between grid points. Convergence criteria included an energy change of $<5 \times 10^{-6}$ eV/atom for scf-cycles, a maximal force of <0.01 eV/Å, and a maximal component of the stress tensor <0.02 GPa.

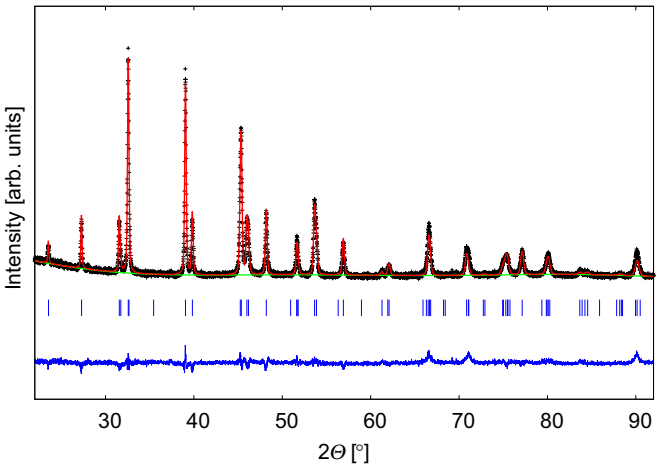

FIG. 2. Powder x-ray diffraction pattern of tetragonal copper sulfide, Cu_2S, at ambient pressure and temperature and Rietveld refinement based on structural data published by Janosi [20] (λ = 1.5406 Å). Black crosses: measured data; red line: simulated pattern; green line: background; blue line: residuals; blue tick marks: calculated reflection positions.

IV. RESULTS

A. Characterization

The product of the synthesis is a polycrystalline compact of opaque copper sulfide which is easily distinguished from the excess copper and the gold capsule [19]. The copper sulfide was separated from the other phases using a diamond wire saw.

The quality of the powder x-ray diffraction data allowed a Rietveld refinement (Fig. 2, Table I) using the structural data published by Janosi [20]. The diffraction data was collected after storing the sample more than 4 months below 260 K. There is no evidence of a transformation into α-chalcocite at this temperature. In accordance with published data for copper sulfides [38] isotropic thermal displacement parameters were fixed at 0.04 Å^2 for copper and at 0.02 Å^2 for sulfur during the refinement. In the final steps of the Rietveld refinement possible preferential orientation was modeled using an eighth-order spherical-harmonic description [39,40].

B. Calorimetry

For the determination of the thermodynamic properties of the low-temperature phase transition the background subtracted excess heat capacity at the transition temperatures was

TABLE I. Crystallographic data for tetragonal copper sulfide, Cu_2S, based on powder x-ray diffraction data.

Author	T [K]	Space group	Z	a [Å]	c [Å]	V [Å^3]
Janosi [20]		$P4_32_12$	4	3.996(2)	11.28(7)	180.1
This study	~293	$P4_32_12$	4	4.003(1)	11.267(1)	180.64(1)
Atom	Wyckoff position	SOF	x	y	z	U_{iso} [Å^2]
Cu (Janosi [20])	8*b*	1	0.34	0.00	0.165	
Cu (this study)	8*b*	1	0.3541(4)	0.0038(4)	0.1672(1)	0.04
S (Janosi [20])	4*a*	1	0.00	0.00	0	
S (this study)	4*a*	1	0.0091(8)	0.0091(8)	0	0.02

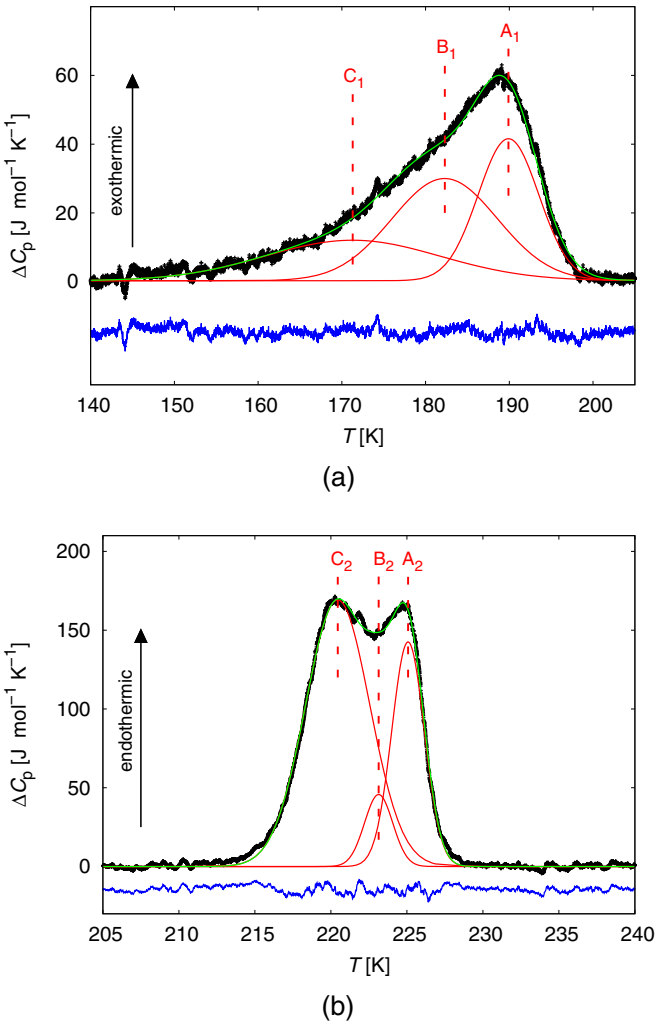

FIG. 3. (a) Fit of the excess heat capacity at the phase transition on cooling. A_1, B_1, C_1: center of Gauss functions; black line: measured data; red line: Gauss functions; green line: calculated model; blue line: residuals; $R^2 = 0.9949$. (b) Fit of the excess heat capacity at the phase transition on heating. A_2, B_2, C_2: center of Gauss functions; black line: measured data; red line: Gauss functions; green line: calculated model; blue line: residuals; $R^2 = 0.9986$.

used, which is shown as a function of temperature on cooling and heating in Figs. 3(a) and 3(b), respectively. For the molar enthalpy of reaction and the molar entropy of reaction we derived values of 1.3(2) kJ mol^{-1} and 6.5(2) J mol^{-1} K^{-1}, respectively.

The temperature dependence of the excess heat capacity during cooling is asymmetric and shows a double peak on heating. The excess heat capacities are well described by three Gauss functions which indicates a multistep process model for the low-temperature phase transition. The transition temperature was derived as the mean value of the centers of the six Gauss functions ($\frac{A_1+B_1+C_1+A_2+B_2+C_2}{6}$) (Table II). According to our data the transition takes place at 202 K with a hysteresis of ±21 K.

The temperature dependence of the heat capacity of tetragonal copper sulfide on cooling between 300 and 2 K using the PPMS is displayed in Fig. 4. The anomaly in

TABLE II. DSC fit data: centers of Gauss functions and transition temperatures.

Cooling	Center [K]	Heating	Center [K]
A_1	189.90(1)	A_2	225.08(1)
B_1	182.3(2)	B_2	223.14(3)
C_1	171.3(9)	C_2	220.45(1)
Mean ($T_{\mathrm{trans},c}$)	181.1(4)	Mean ($T_{\mathrm{trans},h}$)	222.9(1)

the heat capacity detected by DSC was also observed using relaxation calorimetry (RC). No further anomaly was found down to 2 K. For further data analysis the region of the phase transition was omitted due to the failure of the two-τ model to provide accurate heat capacity values across the first-order phase transition as mentioned in the Experimental section. The data can be described by two sixth-order polynomial functions between 2 and 35 K and between 30 and 300 K as shown in

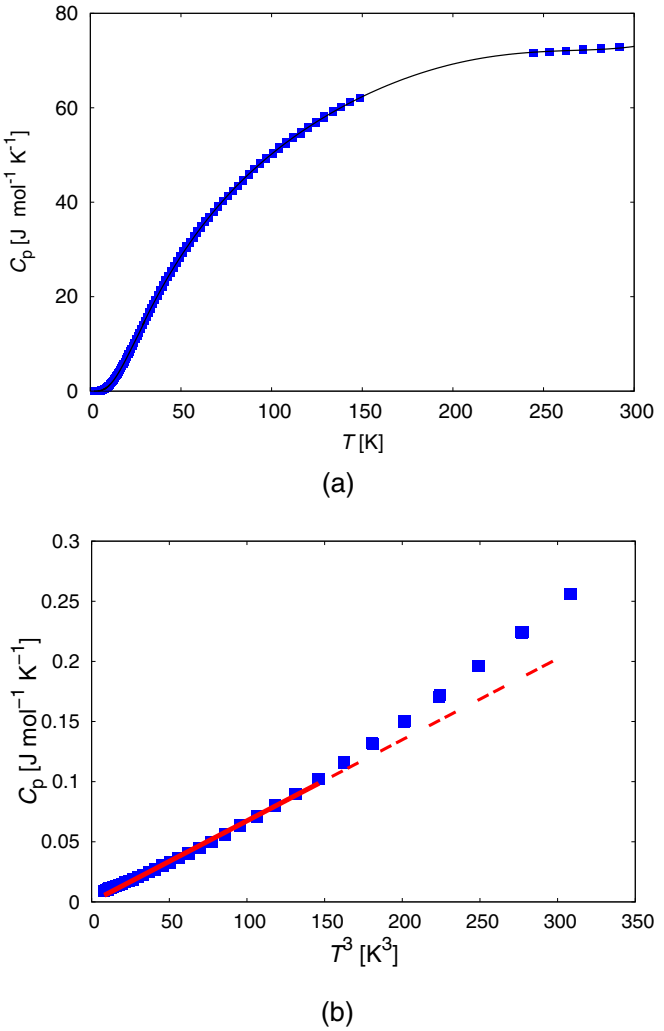

FIG. 4. (a) Heat capacity of tetragonal copper sulfide as a function of temperature on cooling. Blue squares: measured data; black line: fit, sixth-order polynomial function. Error bars smaller than symbol size. (b) Linear fit of the heat capacity based on Eq. (3). The Debye temperature $\theta_D = 205(2)$ K. Blue squares: measured data; red line: calculated model. Error bars smaller than symbol size.

TABLE III. Molar entropy of reaction derived from the excess heat capacity across the phase transition determined by DSC, molar entropy between 300 and 2 K derived from RC data, and the standard molar entropy, S^0.

DSC	Molar entropy of reaction	6.5(2) J mol^{-1} K^{-1}
RC	Molar entropy	115(2) J mol^{-1} K^{-1}
DSC + RC	Standard molar entropy, S^0	122(2) J mol^{-1} K^{-1}

Fig. 4. From the fit between 2 and 300 K a molar entropy of 115(2) J mol^{-1} K^{-1} was calculated. The standard molar entropy, S^0, of tetragonal copper sulfide can be described as the sum of the molar entropy of reaction determined by DSC and the molar entropy derived from RC data as shown in Table III. This description is valid as long as the contributions to the standard molar entropy between 0 and 2 K are negligible. For the determination of the Debye temperature the heat capacity was fitted between 2 and 5 K using Eq. (3) as displayed in Fig. 4. The derived Debye temperature is 205(1) K.

C. X-ray diffraction

At ambient temperature the reflections of the sample were successfully indexed with a threefold twin of tetragonal copper sulfide with an average unit cell of $a = 4.0022(3)$ Å, $c = 11.276(1)$ Å, and $V = 180.61(2)$ Å^3 using single-crystal x-ray diffraction. The threefold twin has a pseudocubic symmetry with $a = 11.29(1)$ Å. The overlap of the reflections (Fig. 5) due to the pseudomerohedral twinning was treated using CRYSALIS^{Pro} [31].

The relation between the three twin domains (D_1,D_2,D_3) (Fig. 6) can approximately be described by the following

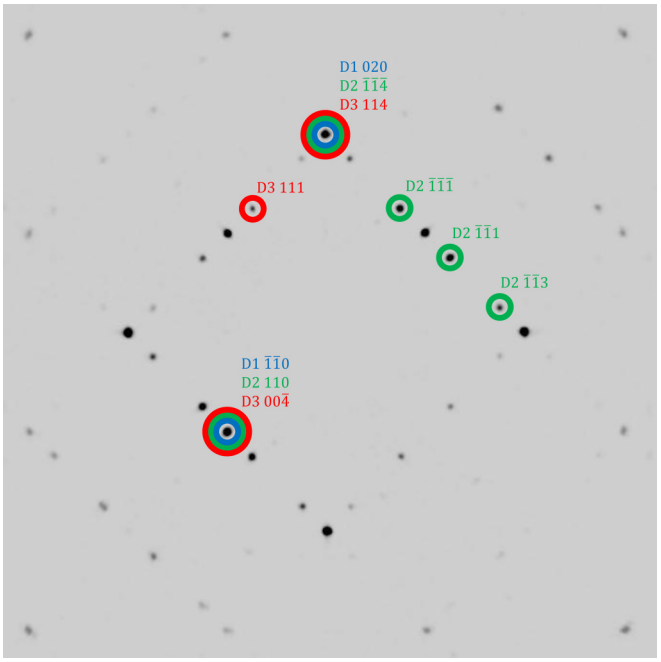

FIG. 5. Reconstructed detector data: reflection overlap of the three twin domains D_1, D_2, and D_3. Software: CRYSALIS^{Pro} [31].

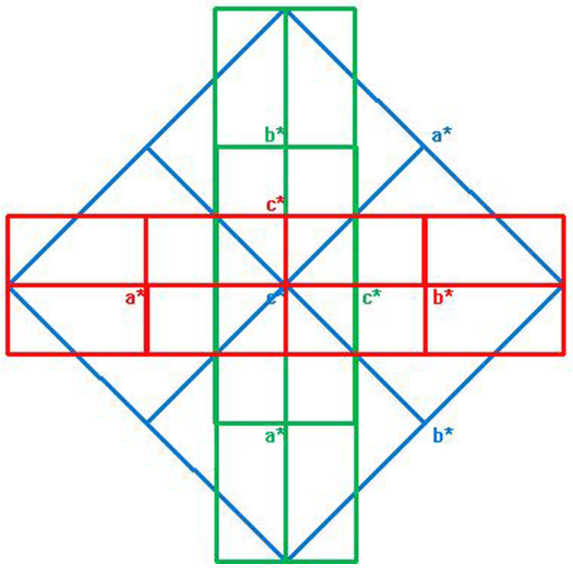

FIG. 6. Orientation of the three twin domains D_1 (blue), D_2 (green), and D_3 (red) in reciprocal space.

rotations in direct space:

D1, D2: 180° rotation around $[\frac{2}{3}; -\frac{2}{3}; \frac{1}{3}]$,

D1, D3: 120° rotation around $[0; 1; \frac{1}{4}]$,

D2, D3: 180° rotation around $[-\frac{2}{3}; -\frac{2}{3}; \frac{1}{3}]$.

The structure was solved in the noncentrosymmetric space group $P4_32_12$ in accordance with the data published by Janosi [20]. Based on the threefold twinning model the atomic positions and their anisotropic displacement parameters were successfully refined [19] (Tables IV and V). The displacement parameters are in good agreement with other published data for copper sulfides showing typically higher values for copper than for sulfur.

At 100 K the reflections of the sample were indexed with an orthorhombic unit cell with $a = 5.3884(7)$ Å, $b = 5.8078(8)$ Å, and $c = 5.7038(6)$ Å. Fifteen space groups were proposed by JANA2006 [33] after performing a space group test. All 15 space groups were included in the process of structure solution and refinement but only the noncentrosymmetric space group $Pna2_1$ (space group 33) yielded a physically reasonable model with acceptable R values. The atomic positions and anisotropic displacement parameters were refined successfully [19] (Tables V, VI). The structure contains 4 formular units of Cu_2S with a theoretical density of 5.9221(9) g/cm^3.

The structure is based on a slightly distorted cubic close packing of sulfur atoms (Fig. 7) similarly to the structure of tetragonal copper sulfide, with two Wyckoff positions for copper. Both copper atoms are coordinated trigonal planar by three sulfur atoms with an average bond length [19] of 2.33(5) Å. For comparison, the average bond length of copper and sulfur in tetragonal copper sulfide [20], chalcocite [38], and djurleite [38] is about 2.30(1) Å, 2.4(2) Å, and 2.30(5) Å, respectively. With sulfur-sulfur distances larger than 3.5 Å and copper-copper distances larger than 2.5 Å the structure fits very well into the scheme of copper sulfide structures [41].

TABLE IV. Crystallographic data for tetragonal copper sulfide, Cu_2S, based on single-crystal XRD data.

T [K]	Space group	Z	a [Å]	c [Å]	V [Å^3]	ρ [g/cm^3]
293(2)	$P4_32_12$	4	4.0022(3)	11.276(1)	180.61(2)	5.8529(1)
Atom	Wyckoff position	SOF	x	y	z	U_{eq} [Å^2]
S	4*a*	1	0.0080(7)	0.0080(7)	0	0.0245(6)
Cu	8*b*	1	0.3590(3)	−0.0068(5)	0.1637(1)	0.0413(5)

As displayed in Fig. 8(a) the powder diffraction pattern of the sample at 100(10) K shows the reflections of the low-temperature phase published previously by Stolen *et al.* [22] besides numerous additional reflections. Recovering the cooled sample back to ambient conditions leads to a complete transformation back into tetragonal copper sulfide according to powder x-ray diffraction experiments [Fig. 8(a)].

For the diffraction pattern at 100(10) K a Rietveld refinement was performed based on the structural data established by single-crystal diffraction experiments for the orthorhombic low-temperature polymorph of tetragonal copper sulfide [19] [Fig. 8(b)]. During the refinement, the isotropic displacement parameters were kept at the values evaluated by single-crystal diffraction. In the final steps of the Rietveld refinement possible preferential orientation was modeled using an eighth-order spherical-harmonic description [39,40]. The average Cu-S bond length in the structure of the orthorhombic low-temperature phase based on the Rietveld refinement is about 2.3(2) Å, which is in good agreement with the average bond length of 2.33(5) established by single-crystal diffraction.

The refinement indicates that the powder pattern consists of reflections of at least two phases. Several reflections which are marked in Fig. 8(b) cannot be explained with the unit cell of the orthorhombic low-temperature phase. Indexations including only the marked reflection as well as indexations including all reflections did not lead to any reliable unit-cell or structural solution. Unidentifiable reflections as a result of low intensity and strong overlap might be the reason for the failure of indexation of a second phase. This also lowers the quality of the Rietveld refinement of the powder pattern based on the structural data for the orthorhombic low-temperature phase.

TABLE V. Parameters and results of single-crystal x-ray diffraction measurements, data reductions, and structural refinements.

Crystal data		
Chemical formula	Cu_2S	Cu_2S
Cell parameters		
a (Å)	4.002(2)	5.385(3)
b (Å)	4.002(2)	5.702(1)
c (Å)	11.276(2)	5.811(4)
V (Å^3)	180.6(2)	178.5(4)
Z	4	4
Space group	$P4_32_12$	$Pna2_1$
Data collection		
Temperature (K)	**293(2)**	**100(5)**
λ (Å)	0.71073	0.71073
Crystal size (μm^3)	50 × 50 × 50	50 × 50 × 50
Reflection range	$-5 \leqslant h \leqslant +5$	$-7 \leqslant h \leqslant +7$
	$-5 \leqslant k \leqslant +5$	$-7 \leqslant k \leqslant +7$
	$-15 \leqslant l \leqslant +15$	$-7 \leqslant l \leqslant +7$
Reflec.	1446	1521
Unique reflec.	324/222	494/449
R_{int}	0.064	0.058
Refinement		
No. of parameters refined	17	29
$R_{obs/all}$	0.048/0.0746	0.051/0.053
$wR_{obs/all}$	0.058/0.0616	0.079/0.079

D. Electrical resistance

Typical results of the electrical resistance measurements of tetragonal copper sulfide samples on cooling and heating are shown in Fig. 9 in comparison to results of Pakeva and Germanova [21]. On cooling the electrical resistance changes by several orders of magnitude in a 20 K interval between 170 and 190 K. On heating a similar behavior is observed but in a smaller interval of about 5 K between 220 and 225 K. These temperatures are in excellent agreement with the temperatures found by DSC measurements for the structural phase transition in tetragonal copper sulfide on cooling and heating. To support this statement the transition temperatures $T_{(trans,c)}$ and $T_{(trans,h)}$ are shown in Fig. 9 as well as the centers of the first (A_1,A_2) and the last (C_1,C_2) reaction peaks of the multistep model derived from DSC measurement data (Table II). The data for the temperature dependence of the resistance of Pakeva and Germanova [21] which were obtained on a phase mixture do not show any sudden change around the transition temperatures (Fig. 9).

The temperature dependence of the conductivity before and after the phase transition can be described by an Arrhenius relation:

$$\sigma = A \exp\left(\frac{-E_a}{k_B T}\right), \tag{4}$$

where A is a preexponential factor, E_a is the activation energy in [eV], k_B is the Boltzmann constant in [eV/K], and T is the absolute temperature in [K].

The relation between conductivity, σ, in [Ω^{-1} m^{-1}] and the electrical resistance, R, in [Ω]

$$\sigma = \frac{1}{Ru} \tag{5}$$

with u as a sample-dependent geometrical factor in [m], allows us to determine the activation energy of the conductivity by deriving the slope from the following linear equation:

$$\ln(1/R) = \ln(A)\frac{-E_a}{k_B}\frac{1}{T} - \ln(1/u) \tag{6}$$

TABLE VI. Crystallographic data for the orthorhombic low-temperature polymorph of Cu_2S from single-crystal XRD data.

T [K]	Space group	Z	a [Å]	b [Å]	c [Å]	V [Å^3]
100(5)	$Pna2_1$	4	5.3884(7)	5.8078(8)	5.7038(6)	178.50(4)
Atom	Wyckoff position	SOF	x	y	z	U_{eq} [Å^2]
S	4a	1	0.2884(8)	0.5299(7)	−0.0980(7)	0.0119(8)
Cu1	4a	1	0.0997(4)	0.2040(3)	0.0433(3)	0.0129(5)
Cu2	4a	1	−0.0576(4)	0.6324(4)	0.1076(3)	0.0164(5)

and multiplying it by $(-k_B)$. The slope was determined by a linear fit of the data points in a $[1/T,\ln(1/R)]$ plot for the tetragonal phase and the low-temperature phase as shown in Fig. 10. From the slope an activation energy of 0.15(2) and 0.22(1) eV was calculated for the tetragonal phase and the low-temperature phase, respectively. These values indicate that conductivity in Cu_2S is mainly due to hydrogenic impurities [42] in both phases with the change in the activation energy E_a being most probably due to the variation in the effective masses of the electrons in the conduction band. We will discuss this point in detail below. Other possible interpretations that could explain the observed decrease of the resistance with temperature, as an increase of the hole mobility, cannot be disregarded. However, in order to explore them we would need to perform Hall effect measurements that are out of the scope of this work.

E. Electronic band structure calculations

Our calculated enthalpy difference in the athermal limit between tetragonal (space group $P4_32_12$) and orthorhombic

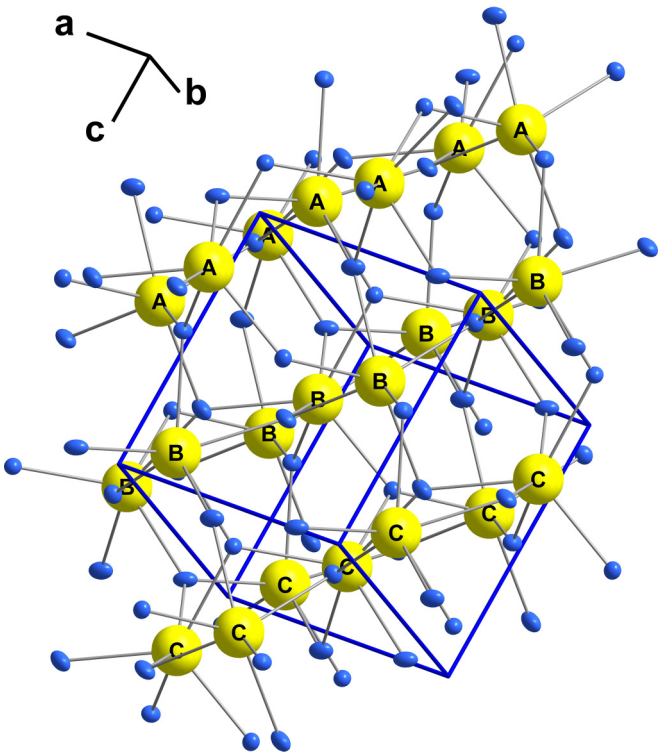

FIG. 7. Crystal structure of the low-temperature polymorph of tetragonal copper sulfide. Black labels on sulfur atoms indicate the slightly distorted cubic close packing of sulfur.

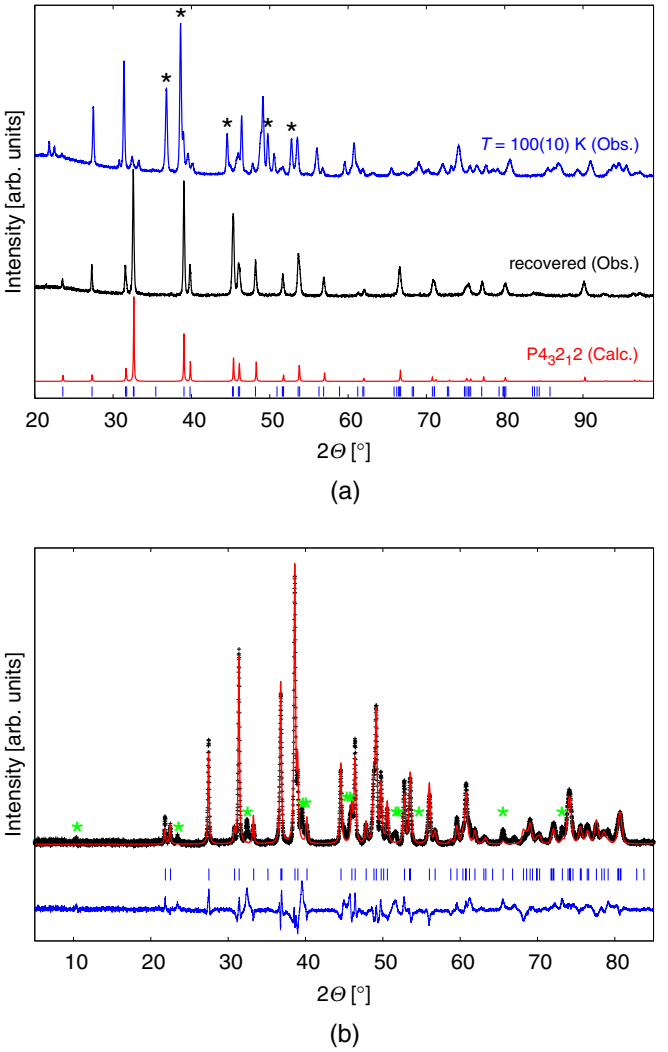

FIG. 8. (a) Blue: diffraction pattern of a sample at 100(10) K. The green stars mark the five reflections published by Stolen *et al.* [22] for the low-temperature polymorph of tetragonal copper sulfide; black: diffraction pattern of a recovered sample at ambient conditions; red: calculated powder diffraction pattern for tetragonal copper sulfide at ambient conditions; blue tick marks: calculated reflection positions for tetragonal copper sulfide at ambient conditions. (b) Powder x-ray diffraction pattern of the orthorhombic low-temperature polymorph at 100(10) K and Rietveld refinement based on structural data established by single-crystal diffraction experiments. Black crosses: measured data; red line: simulated pattern; green line: background; blue line: residuals; blue tick marks: calculated reflection positions; green stars: reflections that cannot be explained by the structural model of the orthorhombic low-temperature polymorph.

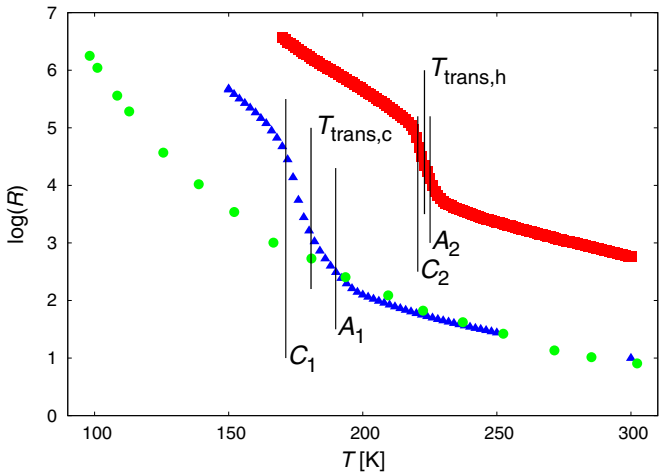

FIG. 9. Logarithm of the electrical resistance of copper sulfide samples as a function of temperature. Red squares: measured data on heating; blue triangles: measured data on cooling; green dots: data from Pakeva and Germanova [21]. Black lines and labels correspond to the transition temperatures determined by differential scanning calorimetry. Error bars smaller than symbol size.

(space group $Pna2_1$) Cu_2S indicates that the low-temperature orthorhombic polymorph is more stable than the ambient temperature tetragonal polymorph consistent with our experimental observations. The deviation between the calculated and experimental lattice parameters in both polymorphs also indicates that our calculations model both polymorphs well (Table VII).

The calculated electronic band structures of both phases are shown in Fig. 11 together with the partial and total electronic density of states (DOS).

In both tetragonal and orthorhombic phases of Cu_2S, and also in the other $Cu_{2-x}S$ polymorphs [43], the top of the valence band is mostly comprised by the Cu d bands while the lowest conduction band is due to the Cu s bands. Thus, electronic transitions to the conduction band are dipole forbidden and will show a weak absorption coefficient α (Fig. 12). Also, the different contribution of the bands results in a valence band with small dispersion due to the high d electron effective masses m_v^* and a conduction band with a small s electron effective mass m_c^* that translates into a high dispersion (Fig. 11). Therefore, while the bottom of the conduction band is perfectly identified in both phases at Γ, the top of the valence band can be tentatively found close to Γ, i.e., in the $M\Gamma$ direction in the case of the ambient temperature tetragonal polymorph and at Γ in the case of the orthorhombic polymorph.

In Fig. 12 we show the optical absorption spectrum at ambient temperature of a 20-μm-thick pellet of tetragonal Cu_2S. With a maximum value of the absorption coefficient of 2000 cm^{-1}, it resembles more an indirect than a direct band gap. However, given that the transition to the conduction band is dipole forbidden, one can expect that an indirect transition, additionally involving a phonon, would not be experimentally observed. This is reinforced by the fact that according to our calculations [Fig. 11(a)], a direct transition at Γ is very close in energy to the indirect one. In Figs. 12(b) and 12(c) we show the energy dependence of the $\ln(\alpha)$ that should be a straight line in the case of a direct band gap explained by Urbach's rule [44] and of the $\alpha^{1/2}$ that should be a straight line for an indirect band gap. In both cases we find a linear dependence; however, the linear range of $\ln(\alpha)$ is longer than with $\alpha^{1/2}$ indicating that the band gap of tetragonal Cu_2S is the direct band gap that calculations find at Γ. Urbach's rule states that the absorption coefficient of a direct band gap tail can be simulated by $\alpha = A_0 \exp[(h\nu - E_g)/E_U]$, where A_0 is an intrinsic constant of the material, E_U is Urbach's energy and relates to the steepness of the absorption edge, and E_g is the band gap. The fit is shown in Fig. 12(a) providing values of $E_g = 1.04(2)$ eV and $E_U = 0.022(2)$ eV. Considering that our calculations determine an indirect band gap $M\Gamma \rightarrow \Gamma$ of 0.494 eV and a direct band gap at Γ of 0.75 eV, we can conclude that, as usually occurs in *ab initio* calculations, our calculations underestimate the direct band gap of tetragonal Cu_2S in 0.29 eV. In the case of the low-temperature orthorhombic phase, the size of the single crystals and the need to use powder pellets prevented us from performing temperature-dependent optical absorption. However, the ground states are accurately determined in our calculations and in both phases the initial

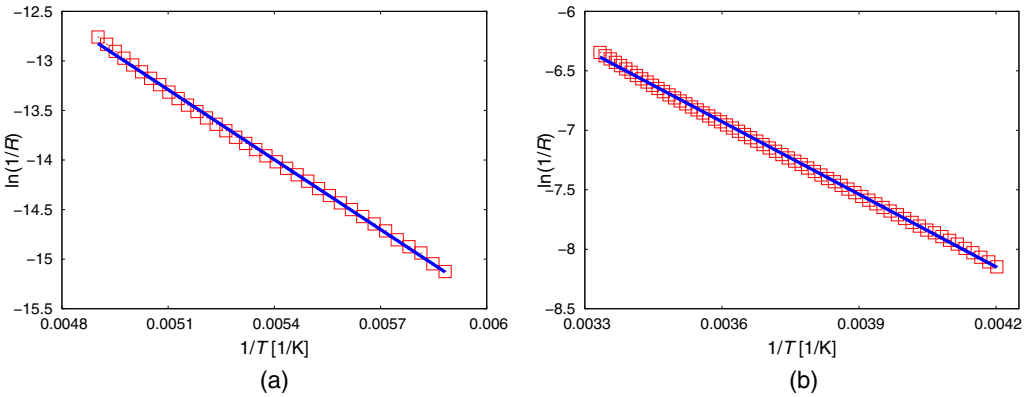

FIG. 10. Linear fit of the natural logarithm of the reciprocal electrical resistance as a function of reciprocal temperature. Using the slope of the linear function of seven and four different datasets an activation energy of the conductivity of 0.15(2) and of 0.22(1) eV was calculated for tetragonal copper sulfide (a) and the low-temperature polymorph (b), respectively. Red open squares: measured data; blue line: linear fit. Error bars smaller than symbol size.

TABLE VII. Lattice parameters for tetragonal and orthorhombic Cu_2S from single-crystal x-ray diffraction and DFT-based calculations.

	Space group	a [Å]	b [Å]	c [Å]	V [Å^3]
Tetr. (expt.)	$P4_32_12$	4.0022(3)	4.0022(3)	11.276(1)	180.61(2)
Tetr. (calc.)	$P4_32_12$	4.0981	4.0981	10.7028	179.745
Orth. (expt.)	$Pna2_1$	5.3884(7)	5.8078(8)	5.7038(6)	178.50(4)
Orth. (calc.)	$Pna2_1$	5.2502	5.9104	5.7514	178.47

and final states are the same. Therefore, we can consider that our calculations make the same underestimation with the band gap of both polymorphs. Thus, the experimental band gap of the low-temperature orthorhombic phase of Cu_2S should be of 0.98 eV.

In Sec. IV D we have found that the activation energy E_a of both tetragonal and orthorhombic phases are 0.15(2) and 0.22(1) eV, respectively. Considering that Cu_2S is a p-type semiconductor and assuming that these values are due to hydrogenic impurities [42], such an increase from the tetragonal to the orthorhombic phase is indicative of an increase of the hole effective mass in the valence band $m^*_{h,v}$ from one phase to the other. Considering the $\boldsymbol{k}\cdot\boldsymbol{p}$ model and a parabolic valence band near the Γ, the effective mass can be deduced [42]:

$$\frac{1}{m^*_{h,c}} = \frac{1}{\hbar^2}\frac{\partial^2 E}{\partial k^2}. \tag{7}$$

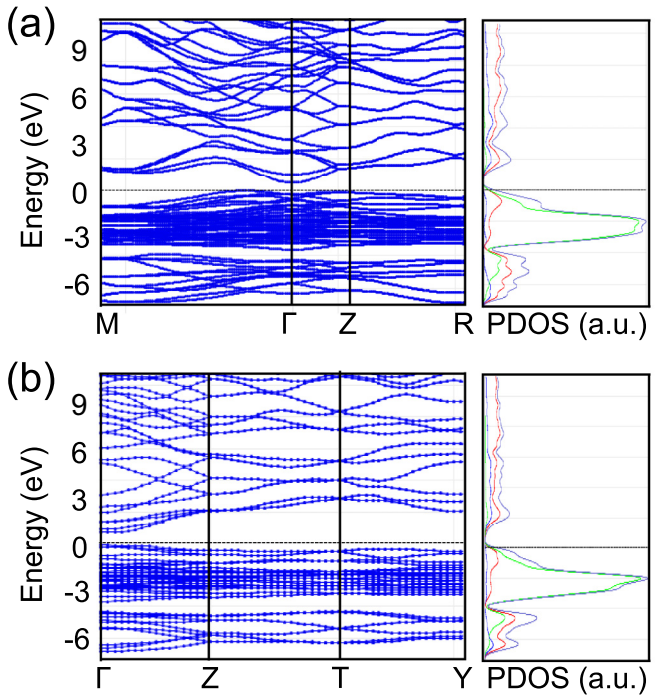

FIG. 11. Electronic band structures and integrated partial density of states (PDOS) of the (a) tetragonal (space group $P4_32_12$) and (b) low-temperature orthorhombic (space group $Pna2_1$) polymorphs of Cu_2S. The continuous blue, red, green, and black lines in the DOS represent the contributions of the Cu s, S p, Cu d, and sum, respectively.

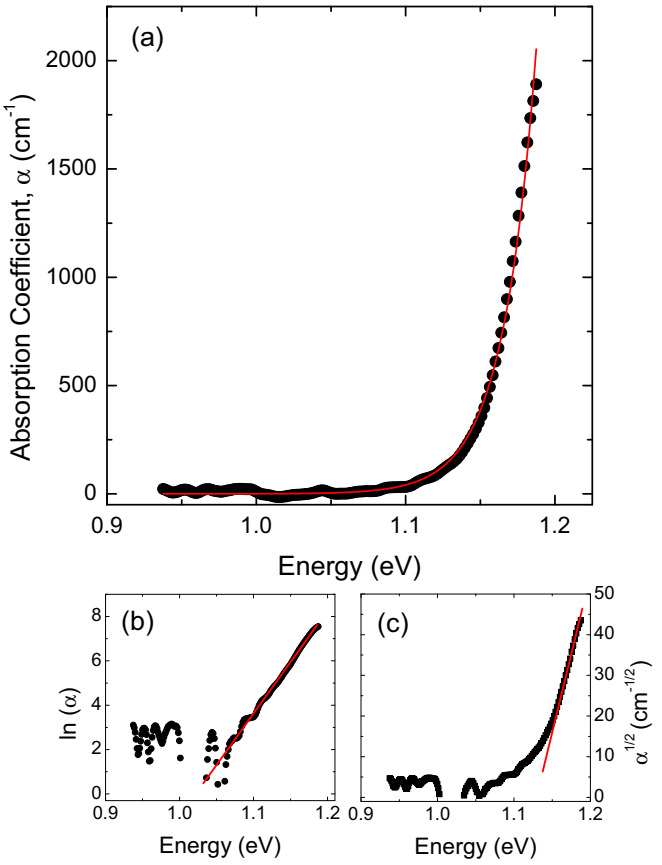

FIG. 12. (a) Optical absorption spectrum (black) of tetragonal Cu_2S at ambient temperature fitted to a direct-type Urbach law [44] (red). Linear range presented by the absorption edge of tetragonal Cu_2S considering either (b) a direct-type Urbach tail [ln(α)] or (c) an indirect ($\alpha^{1/2}$). The points are experimental data while the straight red lines are guides for the eye.

Thus, the smaller the valence band dispersion around Γ, the smaller is the $\partial^2 E/\partial k^2$ and the larger the $m^*_{h,c}$. Since the activation energy E_a is proportional for hydrogenic impurities to $m^*_{h,c}$ the valence band near Γ must show a larger dispersion in the high-temperature tetragonal phase than in the low-temperature orthorhombic phase. In Fig. 11 one can observe, despite the intrinsic low dipersion of the Cu d bands, that this is the case.

V. SUMMARY AND CONCLUSIONS

In this study we synthesized phase-pure, polycrystalline samples and single crystals of tetragonal copper sulfide and solved the structure in space group $P4_32_12$ as proposed by Janosi [20]. We have found a low-temperature-induced tetragonal to orthorhombic phase transition at 202 K by using x-ray diffraction, calorimetry, and resistance measurements on phase-pure samples. The structure of the orthorhombic low-temperature polymorph of Cu_2S has been solved in space group $Pna2_1$ by single-crystal x-ray diffraction. The unit cell of the new phase consits of four formula units of Cu_2S with $a = 5.3884(7)$ Å, $b = 5.8078(8)$ Å, $c = 5.7038(6)$ Å, and $V = 178.50(4)$ Å^3. Similarly to the structure of tetragonal copper sulfide [20], anilite [13], and digenite [12], the structure

of the low-temperature polymorph is based on a slightly distorted cubic close packing of sulfur. In the structure copper is trigonal planar coordinated by three sulfur atoms with an average bond length of 2.33(5) Å.

The local shape of the maxima in the temperature dependence of the heat capacity at the transition temperatures indicates that the structural phase transition from the tetragonal to the orthorhombic polymorph is not a single process. The anomalies are well described by three Gauss functions and therefore might be the result of three processes. Since there is a hysteresis and a significant amount of latent heat at least one of the processes must be of first order. The lack of any group-subgroup relation between the two polymorphs makes it plausible that at least one process has a reconstructive character. Additional reflections found by powder x-ray diffraction at low temperatures that cannot be indexed with the unit cell of the orthorhombic polymorph indicate that another metastable/stable phase is present at low temperatures. This unknown phase might be the result of the multiprocess nature of the observed temperature-induced phase transition. According to the results of relaxation calorimetry no further phase transition takes place down to 2 K since no further anomaly in the heat capacity was observed. The calculated molar entropy of 115(2) J mol^{-1} K^{-1} is similar to the published value of about 116 J mol^{-1} K^{-1} [45] for monoclinic α-chalcocite, Cu_2S. The molar entropy of reaction and the molar enthalpy of reaction of the phase transition differ significantly from that published by Stolen *et al.* [22]. The samples used by Stolen *et al.* [22] contained varying and unquantified amounts of tetragonal copper sulfide depending on the thermal history and therefore leading to varying values since no other copper sulfide phase undergoes this low-temperature phase transition.

The results for the temperature dependence of the electrical resistance indicate that the transition is accompanied by a change in electrical properties. At similar transition temperatures as determined by calorimetric measurements on cooling and heating the electrical resistance of the copper sulfide samples changes by several orders of magnitude. Such a change is not reported by Pakeva and Germanova [21] which might be caused by possible transformation of tetragonal copper sulfide into chalcocite. This known transformation which can reach rates of 1% per day at room temperature [18] was neither discussed nor mentioned in the published study by Pakeva and Germanova [21]. Furthermore, no information was given on the storage time and on the storage conditions of the samples, which might have caused the transformation into chalcocite. However, the value for the activation energy of the conductivity published by Pakeva and Germanova [21] is similar to our findings. For the tetragonal copper sulfide phase and for the orthorhombic low-temperature polymorph an activation energy of the conductivity of 0.15(2) and 0.22(1) eV was determined, respectively. The increase in the activation energies between the polymorphs and the direct nature of the band gap of the tetragonal phase of Cu_2S [$E_g = 1.04(2)$ eV] are discussed by analyzing the calculated electronic band structure of both polymorphs.

ACKNOWLEDGMENTS

Financial support from the Goethe-University Frankfurt am Main, the DFG (Wi 1232), and the BMBF (05K16RFB) is gratefully acknowledged. D.Z. acknowledges Christopher Neun for support with sample preparation. J.R.-F. acknowledges the Spanish MINECO for the Juan de la Cierva (IJCI-2014-20513) Program and for Grants No. MAT2016-75586-C4-1/3-P and No. MAT2015-71070-REDC (MALTA Consolider).

[1] E. Hirahara, J. Phys. Soc. Jpn. **6**, 422 (1951).
[2] F. DiBenedetto, M. Borgheresi, A. Caneschi, G. Chastanet, C. Cipriani, D. Gatteschi, G. Pratesi, M. Romanelli, and R. Sessoli, Eur. J. Mineral. **18**, 283 (2006).
[3] Y. He, T. Day, T. Zhang, H. Liu, X. Shi, L. Chen, and G. J. Snyder, Adv. Mater. **26**, 3974 (2014).
[4] T. Miller, J. Wittenberg, H. Wen, S. Connor, Y. Cui, and A. Lindenberg, Nat. Commun. **4**, 1369 (2013).
[5] R. Hall and J. Meakin, Thin Solid Films **63**, 203 (1979).
[6] S. Choi, W. Yang, K. Kim, Y. Kyoung, J. Chung, H. Bae, J. Park, K. Kim, S. Lee, and S. Cho, Electron. Mater. Lett. **7**, 313 (2011).
[7] D. J. Chakrabarti and D. E. Laughlin, Bull. Alloy Phase Diagr. **4**, 254 (1983).
[8] T. Barth, ZBL Mineral. Geol. **26**, 284 (1926).
[9] H. T. Evans, Nature Phys. Sci. **232**, 69 (1971).
[10] N. Morimoto, Mineral. J. **3**, 338 (1962).
[11] W. G. Mumme, R. W. Gable, and V. Petricek, Can. Mineral. **50**, 423 (2012).
[12] N. W. Buerger, Am. Mineral. **27**, 712 (1942).
[13] N. Morimoto, K. Koto, and H. Shimazaki, Am. Mineral. **54**, 1256 (1969).
[14] S. Djurle, Acta Chem. Scand. **12**, 1415 (1958).
[15] W. van der Stam, A. C. Berends, and C. de Mello Donega, ChemPhysChem **17**, 559 (2016).
[16] L. Liu, C. Liu, W. Fu, L. Deng, and H. Zhong, ChemPhysChem **17**, 771 (2016).
[17] E. H. Roseboom, Jr., Bull. Soc. Econ. Geol. **61**, 641 (1966).
[18] B. J. Skinner, Econ. Geol. **65**, 724 (1970).
[19] See Supplemental Material at http://link.aps.org/supplemental/10.1103/PhysRevB.96.054108 for crystallographic data and a sample picture.
[20] A. Janosi, Acta Crystallogr. **17**, 311 (1964).
[21] S. Pakeva and K. Germanova, J. Phys. D: Appl. Phys. **18**, 1371 (1985).
[22] S. Stolen, F. Gronvold, and E. F. Westrum, Jr., J. Chem. Thermodyn. **22**, 1035 (1990).
[23] A. Rothwarf, Sol. Cells **2**, 115 (1980).
[24] K. L. Chopra and S. R. Das, *Thin Film Solar Cells*, 1st ed. (Plenum, New York, 1983).
[25] A. Putnis, Philos. Mag. **34**, 1083 (1976).
[26] T. Machani, D. P. Rossi, B. J. Golden, E. C. Jones, M. Lotfipour, and K. E. Plass, Chem. Mater. **23**, 5491 (2011).

[27] W. R. J. Cook, *Solid State Chemistry*, Proceedings of the 5th Materials Research Symposium, National Bureau of Standards Special Publication 364 (United States Department of Commerce, Washington, D.C., 1972), p. 703.
[28] H. Rietveld, J. Appl. Crystallogr. **2**, 65 (1969).
[29] A. C. Larson and R. B. Von Dreele, Los Alamos National Laboratory Report, 2000, p. 86.
[30] B. H. Toby, J. Appl. Crystallogr. **34**, 210 (2001).
[31] Agilent, *Crysalis Pro software system*, version 1.171.36.28 (Agilent Technologies UK Ltd., Oxford, UK, 2013).
[32] L. Palatinus and G. Chapuis, J. Appl. Crystallogr. **40**, 786 (2007).
[33] V. Petricek, M. Dusek, and L. Palatinus, Z. Kristallogr. **229**, 345 (2014).
[34] J. C. Lashley, M. F. Hundley, A. Migliori, J. L. Sarrao, P. G. Pagliuso, T. W. Darling, M. Jaime, J. C. Cooley, W. L. Hults, L. Morales *et al.*, Cryogenics **43**, 369 (2003).
[35] P. Hohenberg and W. Kohn, Phys Rev. **136**, B864 (1964).
[36] S. J. Clark, M. D. Segall, C. J. Pickard, P. J. Hasnip, M. I. J. Probert, K. Refson, and M. C. Payne, Z. Kristallogr. **220**, 567 (2005).
[37] H. J. Monkhorst and J. D. Pack, Phys. Rev. B **13**, 5188 (1976).
[38] H. T. J. Evans, Z. Kristallogr. **150**, 299 (1979).
[39] R. B. Von Dreele, J. Appl. Crystallogr. **30**, 517 (1997).
[40] T. Leventouri, Physica C **277**, 82 (1997).
[41] H. T. Evans, Jr., Am. Mineral. **66**, 807 (1981).
[42] P. Y. Yu and M. Cardona, *Fundamentals of Semiconductors: Physics and Materials Properties*, 4th ed. (Springer, New York, 2010).
[43] P. Lukashev, W. R. L. Lambrecht, T. Kotani, and M. van Schilfgaarde, Phys. Rev. B **76**, 195202 (2007).
[44] F. Urbach, Phys. Rev. **92**, 1324 (1953).
[45] F. Gronvold and E. F. Westrum, Jr., J. Chem. Thermodyn. **19**, 1183 (1987).